PROCEEDINGS OF SCIENCE

Recent applications of the gradient flow

Robert Harlander[a,*] **and Andrea Shindler**[a,b,c]

[a] *RWTH Aachen University, Sommerfeldstr. 16, 52074 Aachen, Germany*

[b] *Department of Physics, University of California, Berkeley, California 94720, USA*

[c] *Nuclear Science Division, Lawrence Berkeley National Laboratory, Berkeley, California 94720, USA*

E-mail: harlander@physik.rwth-aachen.de, shindler@physik.rwth-aachen.de

The gradient flow provides a gauge- and O(4)-invariant ultraviolet regulator for QCD. This opens new opportunities for combining non-perturbative lattice calculations with perturbative results, in particular in the context of an operator-product expansion (OPE). We review the concepts behind this and argue that, within the operator basis of a given OPE, the flow-time dependence of the conversion between flowed and regular Wilson coefficients is exact at each perturbative order. Recent applications to parton distribution functions, heavy-meson observables, quark masses, and gradient-flow definitions of the strong coupling are discussed. Finally, the perturbative formulation of the Ricci flow in quantum gravity and its application to the study of non-Gaussian fixed points is reviewed.

Loops and Legs in Quantum Field Theory (LL2026)
12-17, April, 2026
Bayreuth, Germany

*Speaker

© Copyright owned by the author(s) under the terms of the Creative Commons Attribution-NonCommercial-NoDerivatives 4.0 International License (CC BY-NC-ND 4.0) All rights for text and data mining, AI training, and similar technologies for commercial purposes, are reserved. ISSN 1824-8039 . Published by SISSA Medialab.

PoS(LL2026)062

1. Operator product expansion

Let us consider the operator-product expansion (OPE) of a physical operator $R(Q)$ in momentum space:

$$R(Q) = \sum_{n=1}^{N} C_n^{\mathrm{B}}(Q) O_n^{\mathrm{B}} + O(1/Q^{d_{\max}+1}) \equiv C^{\mathrm{B}}(Q) O^{\mathrm{B}} + O(1/Q^{d_{\max}+1}) \,. \tag{1}$$

As an example for $R(Q)$, one may consider a particular Lorentz structure of a current-current operator. The scale Q is assumed to be large compared to any other mass scales, and w.l.o.g., we can also assume $R(Q)$ to be dimensionless; this implies that the sum involves operators of mass dimension $d \le d_{\max}$, and the bare Wilson coefficients C_n^{B} are proportional to $1/Q^{d_n}$, modulo powers of $\ln Q$, where d_n is the mass dimension of the operator O_n^{B}.

In general, neither the Wilson coefficients nor matrix elements of the operators on the r.h.s. are ultraviolet (UV) finite; however, since $R(Q)$ is a physical operator by assumption, the UV divergences must cancel. They can be absorbed into the renormalization and mixing of the operators and the corresponding Wilson coefficients,

$$C^{\mathrm{B}}(Q) = C(Q) Z \,, \qquad O^{\mathrm{B}} = Z^{-1} O \,, \tag{2}$$

such that the *renormalized* Wilson coefficients $C(Q)$ and matrix elements of the *renormalized* operators O are UV finite. Unless stated otherwise, we will assume the renormalization matrix to be in the $\overline{\mathrm{MS}}$ scheme in this paper. It then has the form[1]

$$Z = \mathbb{1} + \sum_{k=1}^{\infty} \sum_{l=1}^{k} c_{kl} \frac{\alpha_s^k}{\epsilon^l} \,, \tag{3}$$

where $\epsilon = (4 - D)/2$, with D the space-time dimension adopted in dimensional regularization.

Both the Wilson coefficients as well as the matrix elements of the composite operators depend on the renormalization scale μ in general,

$$\mu^2 \frac{\mathrm{d}}{\mathrm{d}\mu^2} C(Q) = -C(Q)\gamma \,, \qquad \mu^2 \frac{\mathrm{d}}{\mathrm{d}\mu^2} \langle O \rangle = \gamma \langle O \rangle \,, \tag{4}$$

where

$$\gamma = \left(\mu^2 \frac{\mathrm{d}}{\mathrm{d}\mu^2} Z \right) Z^{-1} \tag{5}$$

is the anomalous dimension matrix of the set of operators O. In matrix elements of the physical operator

$$R(Q) = C(Q) O + O(1/Q^{d_{\max}+1}) \,, \tag{6}$$

the μ-dependence cancels exactly; in perturbation theory, a residual scale dependence remains which is formally of higher order.

Typically, $C(Q)$ is computed perturbatively, while the hadronic matrix elements of O account for the non-perturbative effects. Their combination requires the lattice operators to be renormalized in a suitable scheme, such as RI/MOM [1], RI/SMOM [2, 3], or the Schrödinger functional (SF)

[1] We restrict the discussion to the physical sector of the operator basis, unless stated otherwise.

PoS(LL2026)062

scheme [4–6], and subsequently matched to the scheme used for the Wilson coefficients. This requires dedicated simulations, typically involving off-shell kinematical configurations in the former cases, or finite-volume simulations in the latter.

The calculation of matrix elements of composite operators on the lattice faces a number of conceptual difficulties though. In particular, since the lattice introduces the dimensionful cutoff a^{-1}, UV divergences can appear as inverse powers of the lattice spacing a, leading to so-called power divergences which can be difficult, if not impossible, to control numerically. Additional conceptual problems arise if the operators carry Lorentz indices. The lattice explicitly breaks the O(4) symmetry of continuous Euclidean space-time to the hypercubic group H(4), so that UV divergences are classified according to irreducible representations of H(4). As a consequence, operators belonging to different O(4) irreducible representations may mix if they belong to the same H(4) representation, including mixing with lower-dimensional operators. The gradient flow provides a gauge- and O(4)-invariant continuum regulator for short-distance singularities in composite operators which can be implemented both perturbatively and non-perturbatively on the lattice.

2. Gradient flow

In order to motivate the gradient flow, let us begin by naively removing the high-momentum modes of the fields in the operator in a Wilsonian fashion. For the gauge field of quantum chromodynamics (QCD), we would write this as (we adopt a Euclidean metric throughout this presentation, unless stated otherwise)

$$A_\mu(x) = \int \mathrm{d}^4p\, e^{ipx}\tilde{A}_\mu(p) \quad \to \quad A_\mu(\Lambda,x) = \int \mathrm{d}^4p\, \theta(\Lambda^2-p^2)e^{ipx}\tilde{A}_\mu(p)\,. \tag{7}$$

This cutoff preserves translations and O(4), but its coordinate-space kernel is nonlocal and has power-law tails. Moreover, a naive momentum-space cutoff on the gauge field does not admit a straightforward gauge-covariant generalization to the interacting non-Abelian theory. Instead of the θ function, we could therefore introduce a softer momentum cutoff as

$$A_\mu(t,x) = \int \mathrm{d}^4p\, e^{-tp^2}\, e^{ipx}\tilde{A}_\mu(p) = \int \frac{\mathrm{d}^4y}{(4\pi t)^2}\, \exp\left[-\frac{(x-y)^2}{4t}\right] A_\mu(y)\,, \tag{8}$$

corresponding to Gaussian smearing of the unregularized field with smearing radius $\sqrt{8t}$. Obviously, this field is the unique solution of

$$\partial_t A_\mu(t,x) = \Box A_\mu(t,x)\,, \qquad A_\mu(t=0,x) = A_\mu(x)\,, \tag{9}$$

which is O(4) invariant in Euclidean space: if $A_\mu(t,x')$ is a solution, then so is the transformed field $A'_\mu(t,x)$, where x and x' as well as A and A' are related by an O(4) rotation. Requiring $A_\mu(t,x)$ to transform in the same way under gauge transformations as $A_\mu(x)$, Eq. (9) is obviously not gauge covariant. However, due to the t derivative, the l.h.s. transforms homogeneously,

$$\partial_t A_\mu(t,x) \to U^\dagger(x)\partial_t A_\mu(t,x)U(x)\,, \tag{10}$$

where $U(x) \in \mathrm{SU}(3)$. A gauge-covariant generalization is provided by the QCD gradient-flow equation [7–9]:

$$\partial_t B_\mu(t,x) = D_\nu(t,x)G_{\nu\mu}(t,x)\,, \qquad B_\mu(t=0,x) = A_\mu(x)\,, \tag{11}$$

PoS(LL2026)062

where

$$D_\mu = \partial_\mu + g_{\rm B}[B_\mu, \cdot]\,, \qquad G_{\mu\nu} = \partial_\mu B_\nu - \partial_\nu B_\mu + g_{\rm B}[B_\mu, B_\nu]\,, \tag{12}$$

with $g_{\rm B}$ the bare strong coupling. At tree level, and for $\partial_\mu B_\mu = 0$, Eq. (11) reduces to the heat equation in Eq. (9). Analogously, flowed quark fields are defined through [10]

$$\partial_t \chi(t,x) = D_{\rm F}^2 \chi(t,x)\,, \qquad \chi(t=0,x) = \psi(x)\,, \tag{13}$$

where $D_{{\rm F},\mu} = \partial_\mu + g_{\rm B} B_\mu$.

Correlation functions of operators which are composed of flowed fields, referred to as *flowed operators* in the following, are UV finite for positive flow time once the QCD parameters are renormalized in the regular way [9, 11]. In the usual lattice normalization, no additional renormalization of flowed gauge-field observables is required; in the normalization defined by Eqs. (11) and (12), a factor of Z_g needs to account for the explicit factor of $g_{\rm B}$ though. Flowed fermion fields, on the other hand, require the separate renormalization constant Z_χ [10, 12].

3. Flowed operator product expansion

3.1 General considerations

Assume that one can write $R(Q)$ of Eq. (1) in terms of flowed operators [13–15], i.e.

$$R(Q) = \sum_n \tilde{C}_n(Q,t)\tilde{O}_n(t) + O(1/Q^{d_{\max}+1}) \equiv \tilde{C}(Q,t)\tilde{O}(t) + O(1/Q^{d_{\max}+1})\,. \tag{14}$$

We can determine the relation between the flowed and the unflowed Wilson coefficients by constructing *projectors* onto the unflowed bare operators as [16, 17]

$$P_n[O_m^{\rm B}] = \delta_{nm}\,. \tag{15}$$

These projectors are constructed from suitable matrix elements, potentially including derivatives w.r.t. the external mass scales (masses and momenta), and evaluated with all of these mass scales set to zero. It follows that

$$\tilde{C}(Q,t) = C^{\rm B}(Q)\zeta^{\rm B}(t)^{-1}\,, \tag{16}$$

where we have introduced the bare *matching matrix*

$$\zeta^{\rm B}_{mn}(t) = P_n[\tilde{O}_m(t)]\,. \tag{17}$$

Since t is the only dimensionful scale on the r.h.s., it must be

$$\zeta^{\rm B}_{mn}(t) \sim t^{(d_n - d_m)/2} \sim (\zeta^{\rm B}(t)^{-1})_{mn}\,, \tag{18}$$

modulo logarithmic terms in t. If one evaluates the bare matching matrix via Eq. (17) in dimensional regularization, it contains $1/\epsilon$ poles which, however, can be factorized into the regular renormalization matrix Z, introduced in Eq. (2), as

$$\zeta(t) = \zeta^{\rm B}(t) Z^{-1} \quad \Rightarrow \quad \tilde{C}(Q,t) = C(Q)\zeta(t)^{-1}\,. \tag{19}$$

PoS(LL2026)062

Note that, up to this point, we have not made any assumptions on the magnitude of t. In a lattice calculation of the flowed matrix elements, the relevant short-distance scales are t and the lattice spacing a. The continuum limit is taken at fixed positive t, while at finite lattice spacing the smearing radius should be sufficiently large compared with the cutoff scale, e.g. $\sqrt{8t} \gtrsim a_{\max}$ when several lattice spacings enter the continuum extrapolation. Moreover, at fixed perturbative order, $1/\sqrt{t}$ and Q should not be too different in order to avoid large logarithms in the flowed Wilson coefficients, thus $t = 1/(\kappa Q^2)$, with $\kappa \sim O(1)$. The variation of the final result with a variation of κ may then serve as an estimate of the theoretical uncertainty.

It is important to note that, in the context of the OPE defined in Eq. (1), *the flowed Wilson coefficients defined in Eq.* (19) *are exact functions of* t *at each order in perturbation theory*. Contributions associated with additional powers in t would in general involve higher-dimensional operators beyond the truncated OPE of Eq. (1).

3.2 Adler function

As an application, consider the OPE of the Adler function (neglecting quark-mass effects; for a precise definition, see Ref. [15], for example)

$$D(Q) = D_{\text{pert}}(Q) + C_G^{\text{B}}(Q)\,\langle F_{\mu\nu}F_{\mu\nu}\rangle_0 + O(Q^{-5})\,, \tag{20}$$

where $\langle\cdot\rangle_0$ denotes the vacuum expectation value (VEV); i.e., in Eq. (14), we identify

$$\langle R(s)\rangle_0 = D(Q)\,, \qquad C_1^{\text{B}}(Q) = D_{\text{pert}}(Q)\,, \qquad C_2^{\text{B}}(Q) = C_G^{\text{B}}(Q)\,. \tag{21}$$

Adopting the strategy outlined in Section 3.1, the flowed versions of the composite operators appearing in Eq. (20) can be expressed as[2]

$$\begin{pmatrix} \mathbb{1} \\ Z_g^2 G_{\mu\nu}(t)G_{\mu\nu}(t) \end{pmatrix} = \zeta^{\text{B}}(t) \begin{pmatrix} \mathbb{1} \\ F_{\mu\nu}F_{\mu\nu} \end{pmatrix}, \qquad \zeta^{\text{B}}(t) = \begin{pmatrix} 1 & 0 \\ \zeta_0(t) & \zeta_G^{\text{B}}(t) \end{pmatrix}. \tag{22}$$

Inverting the matching matrix, we find

$$\tilde{C}_1(Q,t) = D_{\text{pert}}(Q) - \zeta_0(t)\, r_G(Q,t)\,, \qquad \tilde{C}_2(Q,t) = r_G(Q,t)\,, \tag{23}$$

where the ratio

$$r_G(Q,t) = \frac{C_G^{\text{B}}(Q)}{\zeta_G^{\text{B}}(t)} \tag{24}$$

is UV finite and known through $O(\alpha_s^2)$ [12, 14, 18–20]. Therefore,

$$D(Q) = \tilde{C}_1(Q,t) + \tilde{C}_2(Q,t)\frac{1}{g^2}E(t) + O(Q^{-5})\,, \tag{25}$$

where $g = g_{\text{B}}/Z_g$ is the renormalized coupling, and

$$E(t) = g_{\text{B}}^2\langle G_{\mu\nu}(t)G_{\mu\nu}(t)\rangle_0 \tag{26}$$

[2]The flowed unit operator is the unit operator.

PoS(LL2026)062

is the flowed gauge action density. As pointed out in Ref. [15], the r.h.s. of Eq. (25) is free from any renormalon ambiguity which typically plagues the r.h.s. of Eq. (20). In order to properly take into account non-perturbative effects, a precise continuum extrapolation of a lattice calculation for $E(t)$ would be desirable in publicly available form.

An important observation is that, in accordance with Eq. (18), $\zeta_0(t) \sim t^{-2}$. At finite perturbative order, this short-distance contribution cannot be expected to cancel exactly against the corresponding contribution contained in a non-perturbative determination of $E(t)$. In the finite-flow-time OPE, $1/\sqrt{t}$ plays the role of a factorization scale and should remain below the hard scale Q, while at fixed perturbative order a very large separation between these scales should be avoided in order to control logarithms of tQ^2. As demonstrated in Ref. [15], there is indeed a rather broad region of flow times where the residual t dependence is weak, providing an important check of the finite-flow-time construction.

3.3 Flow-time evolution

Very often, the typical scales for the operator matrix elements and the Wilson coefficients are widely separated, so that one cannot avoid large logarithms in a fixed-order calculation of the Wilson coefficients. This is true both in the regular as well as the flowed OPE. And similar to the former, it is possible to resum these logarithms in the latter in terms of a renormalization group (RG)-like equation [14, 21],

$$t\partial_t \tilde{C}(Q,t) = -\tilde{C}(Q,t)\tilde{\gamma}(t)\,, \qquad t\partial_t \tilde{O}(t) = \tilde{\gamma}(t)\tilde{O}(t)\,, \tag{27}$$

where

$$\tilde{\gamma}(t) = \left(t\frac{\mathrm{d}}{\mathrm{d}t}\zeta(t)\right)\zeta^{-1}(t)\,, \tag{28}$$

and we would like to point out the formal resemblance to Eqs. (4) and (5). This equation can be solved analogously to the standard RG equation in the $\overline{\text{MS}}$ scheme. Note, however, that as opposed to the latter, Eq. (27) mixes Wilson coefficients corresponding to different mass dimensions in general, i.e.,

$$\tilde{\gamma}_{mn}(t) = \sum_k \left(t\frac{\mathrm{d}}{\mathrm{d}t}\zeta_{mk}(t)\right)\zeta^{-1}(t)_{kn} \sim t^{(d_n-d_m)/2}\,, \tag{29}$$

with the same notation as in Section 3.1. Note that each term in the sum scales as $t^{(d_n-d_m)/2}$, independent of k. Thus, outside of the truncated OPE framework introduced above, the sum over k requires an infinite number of terms. However, within the OPE context, the sum is limited by the finite size of the operator basis, induced via the requirement $d_k \le d_{\max}$. Interestingly, increasing $d_{\max}$ thus changes the elements of $\tilde{\gamma}$; however, it also increases the size of the operator basis. The change in evolution due to one element $\tilde{\gamma}_{mn}$ is thus (partly) compensated by the additional operators in the evolution of the individual $\tilde{C}_n(Q,t)$.

The main message here is that, within the chosen OPE operator basis, $\tilde{\gamma}(t)$ as defined through Eq. (27) is well-defined and *an exact*[3] *function of* t.

[3] It still is a perturbative expression in α_s, of course. For a non-perturbative approach to $\tilde{\gamma}$, see Ref. [22].

PoS(LL2026)062

3.4 Short-flow-time expansion

Instead of converting the $\overline{\text{MS}}$ Wilson coefficients to the flowed scheme as in the previous sections, one may also apply the matching matrix to the flowed operators:

$$O = \zeta^{-1}(t)\tilde{O}(t)\,. \tag{30}$$

In the context of an OPE as in Eq. (1), this is equivalent to the procedure described in Section 3.1, of course, if we consistently expand the expression for $R(Q)$ in α_s.

The main purpose of Eq. (30), though, is to apply it *outside* the context of an OPE, i.e., without having an external UV scale Q in mind, and taking the limit $t \to 0$. In this sense, the r.h.s. should be considered as reconstructing the $\overline{\text{MS}}$-renormalized operator; this is the so-called short-flow-time expansion (SFTX). However, both factors on the r.h.s. of Eq. (30) contain divergences in this limit. The fact that they are calculated using different methods (lattice and perturbation theory) requires, at finite perturbative order and numerical precision, additional efforts to control the cancellation of these divergences. In the case of purely logarithmic divergences, this has been successfully studied in quite some detail, as the examples to be considered below will show. First investigations for the case of power divergences were conducted in Ref. [23].

Recall that in the case of the flowed OPE described in Sections 3.1 and 3.2, the strict limit $t \to 0$ is not required, and thus these practical problems are avoided.

4. Applications

4.1 Parton distribution functions

An obvious goal for any non-perturbative approach to QCD is to describe the properties of hadrons from first principles. The calculation of hadron masses was a milestone achievement in lattice gauge theory [24], which has since developed into a precision tool for Standard Model phenomenology [25, 26]. The parton structure of hadrons, however, still needs to be inferred mostly from experimental data.

The Euclidean formulation of lattice gauge theory is in conflict with the light-cone definition of parton density functions (PDFs). Alternatively, one may consider their Mellin moments,

$$\langle x^n\rangle_{i/h}(\mu) = \int_0^1 \mathrm{d}x\, x^n \left[f_{i/h}(x,\mu) + (-1)^{n+1} f_{\bar{i}/h}(x,\mu)\right], \tag{31}$$

where $f_{i/h}(x,\mu)$ denotes the distribution of a quark of flavor i carrying a fraction x of the momentum of hadron h, and $f_{\bar{i}/h}(x,\mu)$ the corresponding antiquark distribution, at factorization scale μ. These moments can be expressed in terms of hadronic matrix elements of the twist-two operators

$$O^{rs}_{\mu_1\cdots\mu_{n+1}} = \bar{q}^r \gamma_{\{\mu_1} D_{\mu_2}\cdots D_{\mu_{n+1}\}} q^s - \text{traces}\,, \tag{32}$$

where r, s denote quark flavors, D_μ is the covariant derivative, and curly brackets denote symmetrization of the Lorentz indices.

Their direct lattice calculation is complicated at higher moments by the breaking of O(4) symmetry to the hypercubic group H(4), which allows mixing with lower-dimensional operators

PoS(LL2026)062

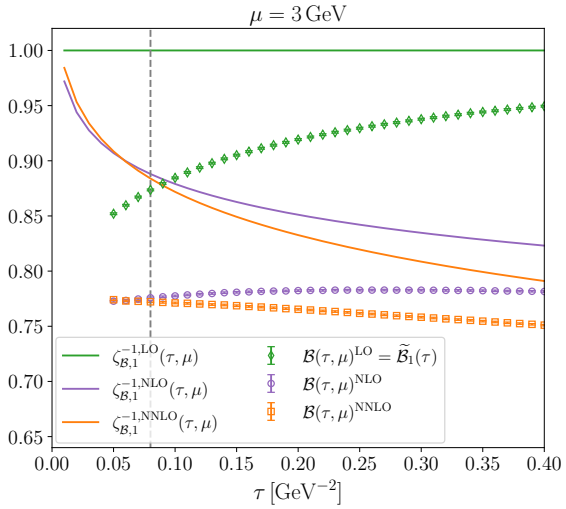

Figure 1: The flowed bag parameter $\tilde{\mathcal{B}}_1(t)$ (green diamonds), the inverse matching coefficient $\zeta_{\mathcal{B},1}^{-1}(t,\mu)$ (solid lines) at leading order (LO) (green), NLO (purple), and NNLO (orange), and their products with $\tilde{\mathcal{B}}_1(t)$ (NLO: purple circles; NNLO: orange squares). The flow time t is denoted as τ in these plots; the renormalization scale is set to $\mu = 3\,\mathrm{GeV}$.

and hence introduces power divergences. This has traditionally restricted calculations with local operators to the lowest moments. Ref. [27] proposed to overcome this limitation using flowed operators: the continuum limit is taken at fixed positive flow time, where O(4) symmetry is restored, thereby eliminating the power-divergent lower-dimensional mixing induced by the reduced lattice symmetry. The flowed matrix elements can subsequently be matched to the physical moments.

For non-singlet flavor configurations, the matching coefficients were obtained through next-to-leading order (NLO) QCD for arbitrary n in Ref. [27], and through next-to-next-to-leading order (NNLO) for $n \leq 5$ [17, 21, 28]. Combined with lattice calculations, this method has enabled the determination of pion PDF moment ratios up to $\langle x^5 \rangle$ and the reconstruction of the pion PDF [29, 30]. A first application of this approach to the gluon momentum fraction $\langle x \rangle_g$ has also been presented in Ref. [31], using the NNLO matching coefficients of Ref. [17]. This exploratory calculation was performed at a single lattice spacing and neglected quark–gluon mixing.

4.2 Heavy meson mixings and lifetimes

The physics of B and D mesons provides sensitive probes of physics beyond the Standard Model. These observables are a classic example of the interplay between perturbative Wilson coefficients and non-perturbative matrix elements of local operators, making them a natural application of the gradient-flow framework discussed above. The non-perturbative contributions are typically parametrized in terms of so-called bag parameters, which are combined with suitable perturbative Wilson coefficients to obtain the physical predictions for lifetimes or mixing parameters.

As an example, Fig. 1 illustrates the extraction of the bag parameter $\mathcal{B}_1(\mu)$ related to the mixing of a fictitious neutral D_s meson into its anti-particle using the gradient flow. The flowed bag parameter $\tilde{\mathcal{B}}_1(t)$ is constructed from matrix elements of flowed four- and two-quark operators;

PoS(LL2026)062

see Ref. [32, 33] for details. The relevant point here is that $\tilde{\mathcal{B}}_1(t)$ can be related to its $\overline{\text{MS}}$ value by using Eq. (30),

$$\mathcal{B}_1(\mu) = \lim_{t\to 0} \zeta^{-1}_{\mathcal{B},1}(t,\mu)\tilde{\mathcal{B}}_1(t)\,, \tag{33}$$

where we have made the μ-dependence explicit. For the particular bag parameter $\mathcal{B}_1$ considered here, the relevant matching relation reduces to a single coefficient $\zeta_{\mathcal{B},1}(t,\mu)$, known through NNLO QCD [21, 34]. Figure 1 shows the flowed lattice bag parameter, the inverse perturbative matching coefficient, and their product at NLO and NNLO. While the weaker flow-time dependence of the NLO result may appear preferable at first sight, the leading corrections neglected in the SFTX are parametrized by terms starting linearly in t in the fits. In any case, both the NLO and the NNLO results allow for a consistent continuum extrapolation at fixed positive flow time followed by an extrapolation to $t \to 0$; for details, see Ref. [32, 33].

4.3 Quark masses

An even simpler application which involves only two-quark operators is the extraction of the quark mass $m(\mu)$ in the $\overline{\text{MS}}$ scheme from lattice data. Starting from the PCAC relation and taking the large Euclidean-time, ground-state limit, one derives

$$\frac{M_\pi}{2}\frac{\langle A_4(x_4)P(0)\rangle_0}{\langle P(x_4)P(0)\rangle_0} = m_{\text{B}}^{\text{PCAC}}\,, \tag{34}$$

where $P(x_4)$ and $A_\mu(x_4)$ are the bare non-singlet zero-momentum pseudoscalar density and axial current at Euclidean time x_4, M_π is the pion mass, and $m_{\text{B}}^{\text{PCAC}}$ is the bare PCAC mass. Replacing these operators by their flowed counterparts in the corresponding ratio, where the flowed-quark field renormalization cancels, defines a UV-finite gradient-flow version of the quark mass, which is related to the $\overline{\text{MS}}$ mass as

$$m(\mu) = \lim_{t\to 0} \zeta_P(t,\mu)\zeta_A(t,\mu)^{-1}\tilde{m}(t)\,, \tag{35}$$

where ζ_A and ζ_P are the matching coefficients for the axial current and pseudoscalar density, renormalized in the $\overline{\text{MS}}$ scheme. The method has been applied successfully to the strange- and charm-quark masses in Ref. [35]. For an alternative way to evaluate $\overline{\text{MS}}$ quark masses from the lattice using gradient flow observables, see Ref. [36, 37].

5. Gradient flow coupling

5.1 Quantum chromodynamics

The flowed gauge action density introduced in Eq. (26) has been a central object for applications of the gradient flow ever since the seminal paper on the gradient flow by M. Lüscher [9]. Aside from its role in scale setting on the lattice, it provides a renormalization scheme for the strong coupling which is accessible perturbatively and on the lattice:

$$\tilde{\alpha}_s(\mu) = \frac{4\pi}{3}t^2E(t)\Big|_{t=c/\mu^2}\,. \tag{36}$$

The parameter c is in principle arbitrary, but is typically set to $1/8$, corresponding to $\mu = 1/\sqrt{8t}$. The perturbative conversion to the $\overline{\text{MS}}$ scheme is known through NNLO and shows good perturbative

PoS(LL2026)062

behavior down to scales of order 1 GeV [12, 19, 37].[4] Comparing to a continuum-extrapolated lattice evaluation of $E(t)$ with $n_f = 3$ flavors, Ref. [39] derives the $\overline{\text{MS}}$ value $\alpha_s^{(5)}(M_Z) = 0.1161^{+0.0027}_{-0.0016}$, compatible with the world average of this quantity, with a somewhat larger uncertainty.

Interestingly, the first non-universal coefficient of the β function in the gradient-flow scheme is considerably larger than in the $\overline{\text{MS}}$ scheme [40–42]. This suggests a more limited perturbative regime for extractions based on this β function, and may require lattice data down to very small values of t [42]. It also motivates the calculation of the next perturbative term which, however, corresponds to a four-loop calculation.

As opposed to the $\overline{\text{MS}}$ scheme which is mass independent and requires explicit matching relations for the transition from QCD with n_f flavors to $n_f \pm 1$ flavors, the gradient-flow scheme implements this decoupling in a natural way. Using the results of Ref. [19] which include the quark mass effects in $E(t)$ through NLO, one finds for the one-loop coefficient of the β function[5]

$$\tilde{\beta}_0 = 11 - \frac{2}{3}\sum_q \left(1 + t\partial_t \Omega_{1q}\right)_{t=c/\mu^2} , \tag{37}$$

where Ω_{1q} is a function of the dimensionless combination $m_q^2 t$. The term in brackets of Eq. (37) is shown in Fig. 2 for $m_q = 5\,\text{GeV}$; from Ref. [19], one derives that it obeys the following limits:

$$1 + t\partial_t \Omega_{1q} \to \begin{cases} 1 & \text{for } m_q \to 0\,, \\ 0 & \text{for } m_q \to \infty\,. \end{cases} \tag{38}$$

Thus, in the case of n_f massless and otherwise only infinitely heavy quarks, it is $\tilde{\beta}_0 = 11 - 2n_f/3$, in agreement with the universal result for mass independent schemes. As one lowers one of the heavy quark masses m_q, $\tilde{\beta}_0$ continuously decreases until it reaches $\tilde{\beta}_0 = 11 - 2(n_f + 1)/3$ at $m_q = 0$. Let us point out that an alternative perturbative definition of the QCD β function which interpolates smoothly across the thresholds has recently been introduced in Ref. [43].

The fact that the gradient flow (GF) scheme is mass dependent has another interesting consequence. While the RG evolution in the $\overline{\text{MS}}$ scheme is governed by logarithmic divergences only, so that power-law sensitivity to dimensionful parameters is not manifest in the running, the mass-dependent GF scheme also retains sensitivity to such power-law effects. This will become relevant in the subsequent discussion.

5.2 Quantum electrodynamics

As mentioned in Section 5.1, the perturbative behavior of the first non-universal coefficient of the GF β function motivates further investigation. One option is to consider the case of quantum electrodynamics (QED), for which the flow equation is linear in the gauge field and can be solved exactly in momentum space. Because of this, the flowed QED action density can be expressed as a Laplace transform of the ordinary photon vacuum-polarization function [44]. Since the latter is known to four-loop level in QED, it is possible to evaluate the QED coupling in the GF scheme to the

[4] A finite-volume evaluation of $E(t)$ using numerical stochastic perturbation theory through NNLO was obtained in Ref. [38].

[5] Thanks to H. Werthenbach for motivating this study. The analysis could also be taken to the two-loop level using the results of Ref. [37].

PoS(LL2026)062

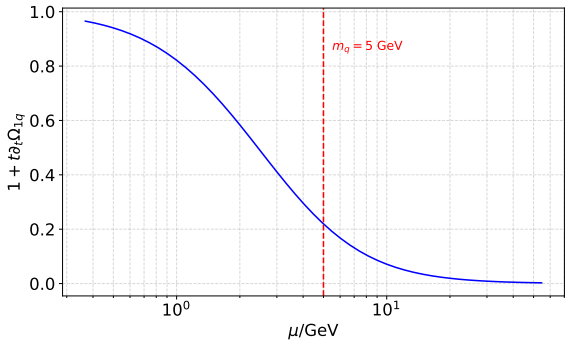

Figure 2: The function $1 + t\partial_t\Omega_{1q}$ which governs the quark contributions to the one-loop β function in the GF scheme. Here, $t = 1/(8\mu^2)$, and $m_q = 5\,\text{GeV}$.

same order (which would correspond to a five-loop calculation performed directly in the gradient-flow formalism). It turns out that the perturbative behavior of the corresponding β function is comparable to that in the $\overline{\text{MS}}$ scheme, which suggests that the features observed in QCD are of non-Abelian origin.

Another interesting application of the QED GF coupling is to study the RG structure of QED_3, i.e., QED in three space-time dimensions. It is well known that QED_3 shares several qualitative features with four-dimensional QCD, including strong infrared dynamics and, for suitable n_f, chiral symmetry breaking. The gradient flow provides an independent tool to study such features. For example, in the large-n_f limit it reproduces both the ultraviolet and infrared fixed points of QED_3 [44]. Non-perturbative investigations of this system could provide further insight in this respect.

6. Ricci flow

As already pointed out in Section 5.1, one of the virtues of the GF scheme compared to the $\overline{\text{MS}}$ scheme is the scale-dependent renormalization condition which makes the RG structure sensitive to power-law effects associated with dimensionful parameters. It was pointed out in Ref. [43] that this is crucial in the context of gravity, where non-perturbative studies provide evidence for a non-Gaussian fixed point underlying the asymptotic-safety scenario for quantum gravity (see, e.g., Ref. [45]). At the same time, Ref. [43] introduced a non-minimal generalization of the $\overline{\text{MS}}$ scheme which preserves sensitivity to such power-law effects and indeed recovers a non-Gaussian fixed point.

From the discussion of the gradient flow in QCD, it is suggestive to introduce a GF-like coupling in gravity and to study its associated RG behavior. For the sake of simplicity, we only consider pure gravity without any matter fields. The only dynamical field in this case is the metric tensor, and it is natural to define a flow equation analogous to Eq. (11) as

$$\partial_t \tilde{g}_{\mu\nu}(t) = -2\tilde{R}_{\mu\nu}(t)\,, \tag{39}$$

where $\tilde{R}_{\mu\nu}(t)$ is the flowed version of the Ricci tensor. With the conventional negative sign, the linearized flow around flat space has a diffusive character and exponentially suppresses high-

PoS(LL2026)062

momentum modes. The factor 2 is the conventional normalization of the Ricci-flow equation introduced by Hamilton [46] and later brought to fame by Perelman as a tool to prove the Poincaré conjecture [47–49].

A perturbative formulation of the Ricci flow in quantum gravity was recently developed in Ref. [50]. The metric, both flowed and unflowed, was expanded around a constant, flat background,

$$g_{\mu\nu}(x) = \delta_{\mu\nu} + h_{\mu\nu}(x)\,, \qquad \tilde{g}_{\mu\nu}(t,x) = \delta_{\mu\nu} + \tilde{h}_{\mu\nu}(t,x)\,, \tag{40}$$

with $h_{\mu\nu}$, $\tilde{h}_{\mu\nu}$ the unflowed and flowed graviton fields. The unflowed Feynman rules of quantum gravity were supplemented by the flowed graviton propagator, graviton flow lines, and the corresponding vertices, taking into account suitable gauge fixing terms for the flowed graviton.

Since Newton's coupling G_N is dimensionful, perturbative Einstein gravity is non-renormalizable by power counting and requires higher-dimensional counterterms. At NLO, these may be represented by terms of the form R^2 and $R_{\mu\nu}R^{\mu\nu}$. In flowed gravity, the corresponding counterterms receive contributions from the UV divergences of the unflowed Green's functions, as well as from divergences associated with the flowed fields at vanishing flow time. Once determined, they allow one to evaluate VEVs of composite operators, for example, in analogy to what is used in QCD in order to define the coupling or the flowed quark mass [9, 12, 36]. In order to arrive at diffeomorphism invariant quantities, it was suggested to integrate these quantities over all space:

$$\mathcal{I}_n(t) = \frac{1}{V}\int \mathrm{d}^D x\sqrt{\tilde{g}(t,x)}\tilde{O}_n(t,x)\,, \tag{41}$$

where V denotes the classical reference volume. Ref. [50] considered the simplest two cases, $\tilde{O}_1 = \mathbb{1}$ and $\tilde{O}_R = \tilde{R}$. Both $\mathcal{I}_1$ and $\mathcal{I}_R$ were found to be finite at two-loop level by the same one-loop counterterms. In the $\overline{\mathrm{MS}}$ scheme, they are not RG invariant though, and their perturbative results depend on the renormalization scale μ. This is problematic if one aims for a comparison to a future non-perturbative implementation of the Ricci flow (RF), for example. A similar situation exists in QCD due to the requirement of a flowed-quark field renormalization. It was resolved by defining the so-called ringed scheme [51], which fixes this renormalization in terms of a specific VEV.

Analogously, Ref. [50] suggested to fix the gravity counterterms such that $\mathcal{I}_1$ does not receive higher-order corrections. Since $V\mathcal{I}_1$ is the volume of the D-dimensional quantum system, this scheme was dubbed the *fixed-volume scheme (FVS)*. In the FVS, $\mathcal{I}_1$ is RG invariant by construction, but also $\mathcal{I}_R$ becomes μ independent. In analogy to Eq. (36), a possible definition of Newton's coupling in the *RF scheme* is then

$$g_\mathrm{RF}(\mu) = -\frac{4t}{3}\mathcal{I}_R^\mathrm{FVS}\Big|_{t=e^{-\gamma_\mathrm{E}}/\mu^2}\,. \tag{42}$$

It turns out that this choice indicates both a perturbatively valid conversion between $g_\mathrm{RF}(\mu)$ and G_N as well as a perturbatively well-behaved β function. At the perturbative order considered, the latter exhibits a UV fixed point at $g_\mathrm{RF} = 4/5$, with associated critical exponent $\theta = 2$, close to values derived from functional renormalization-group methods [52].

It remains to be seen whether the observations within RF gravity remain stable against higher-order perturbative corrections, which, however, turn out to be much more difficult to obtain than in flowed QCD. Furthermore, it might be worth implementing the Ricci flow in non-perturbative

PoS(LL2026)062

approaches to quantum gravity such as Causal Dynamical Triangulation or Euclidean Dynamical Triangulation,[6] providing an independent test of the perturbative result.

7. Conclusions

We have collected a personally biased subset of recent developments in the gradient flow, reflecting its increasing range of applications. Due to space limitations, some important recent results had to be left out, in particular the NLO matching of *low-energy effective field theory (LEFT)* operators to their flowed counterparts [55], or the application of the gradient flow to scalar QCD [56]. We reviewed the concept of a flowed OPE [13, 15], where the flow time introduces an additional scale which is kept at finite positive values, and the strict $t \to 0$ limit is not required. Within the truncated OPE, the resulting flowed Wilson coefficients are exact functions of the flow time at each perturbative order, and their flow-time evolution is governed by the flowed anomalous dimension. Applications to parton distributions, heavy-meson observables, quark masses, and gradient-flow couplings illustrate the versatility of this framework. Finally, we discussed the Ricci flow as a natural gravitational analogue of the gradient flow and its recent perturbative application to the study of a non-Gaussian fixed point in quantum gravity.

Acknowledgments. We are indebted to all our students, postdocs, and colleagues for advancing the applications and understanding of the gradient flow. Some of the insights presented in these proceedings were inspired by discussions with participants at the 2026 Gradient Flow Workshop in Edinburgh. R.H. would like to thank the organizers of Loops&Legs for the invitation to present the gradient flow, and acknowledges support from the *German Research Foundation (DFG)* through grants 513989149 and 396021762 (TRR 257 "Particle Physics Phenomenology after the Higgs Discovery"); A.S. acknowledges support from *National Science Foundation* under grant PHY-2209185.

References

[1] G. Martinelli, C. Pittori, C. T. Sachrajda, M. Testa, and A. Vladikas, *A general method for non-perturbative renormalization of lattice operators*, *Nucl. Phys. B* **445** (1995) 81–108, arXiv:hep-lat/9411010.

[2] Y. Aoki *et al.*, *Nonperturbative renormalization of quark bilinear operators and B_K using domain wall fermions*, *Phys. Rev. D* **78** (2008) 054510, arXiv:0712.1061 [hep-lat].

[3] C. Sturm, Y. Aoki, N. H. Christ, T. Izubuchi, C. T. C. Sachrajda, and A. Soni, *Renormalization of quark bilinear operators in a momentum-subtraction scheme with a nonexceptional subtraction point*, *Phys. Rev. D* **80** (2009) 014501, arXiv:0901.2599 [hep-ph].

[4] M. Lüscher, P. Weisz, and U. Wolff, *A Numerical method to compute the running coupling in asymptotically free theories*, *Nucl. Phys. B* **359** (1991) 221–243.

[6] For reviews, see Refs. [53, 54], for example.

PoS(LL2026)062

[5] M. Lüscher, R. Narayanan, P. Weisz, and U. Wolff, *The Schrödinger functional: A renormalizable probe for non-Abelian gauge theories*, *Nucl. Phys. B* **384** (1992) 168–228, arXiv:hep-lat/9207009.

[6] S. Sint, *On the Schrödinger functional in QCD*, *Nucl. Phys. B* **421** (1994) 135–158, arXiv:hep-lat/9312079.

[7] R. Narayanan and H. Neuberger, *Infinite N phase transitions in continuum Wilson loop operators*, *JHEP* **03** (2006) 064, arXiv:hep-th/0601210.

[8] M. Lüscher, *Trivializing maps, the Wilson flow and the HMC algorithm*, *Commun. Math. Phys.* **293** (2010) 899–919, arXiv:0907.5491 [hep-lat].

[9] M. Lüscher, *Properties and uses of the Wilson flow in lattice QCD*, *JHEP* **08** (2010) 071, arXiv:1006.4518 [hep-lat]. [Erratum: JHEP 03, 092 (2014)].

[10] M. Lüscher, *Chiral symmetry and the Yang–Mills gradient flow*, *JHEP* **04** (2013) 123, arXiv:1302.5246 [hep-lat].

[11] M. Lüscher and P. Weisz, *Perturbative analysis of the gradient flow in non-abelian gauge theories*, *JHEP* **02** (2011) 051, arXiv:1101.0963 [hep-th].

[12] J. Artz, R. V. Harlander, F. Lange, T. Neumann, and M. Prausa, *Results and techniques for higher order calculations within the gradient-flow formalism*, *JHEP* **06** (2019) 121, arXiv:1905.00882 [hep-lat]. [Erratum: JHEP 10, 032 (2019)].

[13] C. Monahan and K. Orginos, *Locally smeared operator product expansions in scalar field theory*, *Phys. Rev. D* **91** no. 7, (2015) 074513, arXiv:1501.05348 [hep-lat].

[14] R. V. Harlander, F. Lange, and T. Neumann, *Hadronic vacuum polarization using gradient flow*, *JHEP* **08** (2020) 109, arXiv:2007.01057 [hep-lat].

[15] M. Beneke and H. Takaura, *Gradient-flowed operator product expansion without IR renormalons*, *JHEP* **03** (2026) 033, arXiv:2510.12193 [hep-ph].

[16] S. G. Gorishnii, S. A. Larin, and F. V. Tkachov, *The algorithm for OPE coefficient functions in the MS scheme*, *Phys. Lett. B* **124** (1983) 217–220.

[17] R. V. Harlander, Y. Kluth, and F. Lange, *The two-loop energy–momentum tensor within the gradient-flow formalism*, *Eur. Phys. J. C* **78** no. 11, (2018) 944, arXiv:1808.09837 [hep-lat]. [Erratum: Eur.Phys.J.C 79, 858 (2019)].

[18] R. Harlander, *Quarkmasseneffekte in der Quantenchromodynamik und asymptotische Entwicklung von Feynman-Integralen*, PhD thesis, 1998. Shaker Verlag.

[19] R. V. Harlander and T. Neumann, *The perturbative QCD gradient flow to three loops*, *JHEP* **06** (2016) 161, arXiv:1606.03756 [hep-ph].

PoS(LL2026)062

[20] R. Brüser, A. H. Hoang, and M. Stahlhofen, *Three-loop OPE Wilson coefficients of dimension-four operators for (axial-)vector and (pseudo-)scalar current correlators*, *JHEP* **12** (2024) 103, arXiv:2408.03989 [hep-ph].

[21] J. Borgulat, R. V. Harlander, J. T. Kohnen, and F. Lange, *Short-flow-time expansion of quark bilinears through next-to-next-to-leading order QCD*, *JHEP* **05** (2024) 179, arXiv:2311.16799 [hep-lat].

[22] M. Black, A. Hasenfratz, and O. Witzel, *Gradient Flow Renormalization Schemes for Composite Fermion Operators*, arXiv:2607.00493 [hep-lat].

[23] SymLat, J. Kim, T. Luu, M. D. Rizik, and A. Shindler, *Nonperturbative renormalization of the quark chromoelectric dipole moment with the gradient flow: Power divergences*, *Phys. Rev. D* **104** no. 7, (2021) 074516, arXiv:2106.07633 [hep-lat].

[24] BMW, S. Dürr *et al.*, *Ab-Initio Determination of Light Hadron Masses*, *Science* **322** (2008) 1224–1227, arXiv:0906.3599 [hep-lat].

[25] ALPHA, M. Dalla Brida, R. Höllwieser, F. Knechtli, T. Korzec, A. Ramos, S. Sint, and R. Sommer, *The strength of the interaction between quarks and gluons*, *Nature* **652** no. 8109, (2026) 328–334, arXiv:2501.06633 [hep-ph].

[26] Flavour Lattice Averaging Group (FLAG), Y. Aoki *et al.*, *FLAG review 2024*, *Phys. Rev. D* **113** no. 1, (2026) 014508, arXiv:2411.04268 [hep-lat].

[27] A. Shindler, *Moments of parton distribution functions of any order from lattice QCD*, *Phys. Rev. D* **110** no. 5, (2024) L051503, arXiv:2311.18704 [hep-lat].

[28] R. V. Harlander, J. T. Kohnen, and A. Shindler, *Short-flow-time expansion of non-singlet twist-two operators at next-to-next-to-leading order QCD*, *Eur. Phys. J. C* **86** no. 4, (2026) 439, arXiv:2511.17145 [hep-ph].

[29] A. Francis *et al.*, *Gradient Flow for Parton Distribution Functions: First Application to the Pion*, *Phys. Rev. Lett.* **136** no. 17, (2026) 171903, arXiv:2509.02472 [hep-lat].

[30] A. Francis, P. Fritzsch, R. Karur, J. Kim, G. Pederiva, D. A. Pefkou, A. Rago, A. Shindler, A. Walker-Loud, and S. Zafeiropoulos, *Moments of parton distribution functions of the pion from lattice QCD using gradient flow*, *Phys. Rev. D* **113** no. 7, (2026) 074520, arXiv:2510.26738 [hep-lat].

[31] HadStruc, R. Edwards, J. Karpie, L. Maio, C. J. Monahan, K. Orginos, D. Richards, A. M. Sturzu, and S. Zafeiropoulos, *Accessing the gluon momentum fraction of nucleons through the gradient flow*, *Phys. Rev. D* **114** no. 1, (2026) 014516, arXiv:2602.14260 [hep-lat].

[32] M. Black, R. V. Harlander, J. T. Kohnen, F. Lange, A. Rago, A. Shindler, and O. Witzel, *Bag Parameters for Heavy Meson Lifetimes*, arXiv:2603.28516 [hep-ph].

[33] M. Black, R. V. Harlander, J. T. Kohnen, F. Lange, A. Rago, A. Shindler, and O. Witzel, *Heavy-Meson Bag Parameters using Gradient Flow*, arXiv:2603.28517 [hep-lat].

PoS(LL2026)062

[34] R. V. Harlander and F. Lange, *Effective electroweak Hamiltonian in the gradient-flow formalism*, *Phys. Rev. D* **105** no. 7, (2022) L071504, arXiv:2201.08618 [hep-lat].

[35] M. Black, R. V. Harlander, A. Hasenfratz, A. Rago, and O. Witzel, *Renormalized quark masses using gradient flow*, *Phys. Rev. D* **113** no. 9, (2026) 094504, arXiv:2506.16327 [hep-lat].

[36] H. Takaura, R. V. Harlander, and F. Lange, *A new approach to quark mass determination using the gradient flow*, *JHEP* **09** (2025) 025, arXiv:2506.09537 [hep-lat].

[37] R. V. Harlander and R. H. Mason, *Quark-mass effects in gradient-flow observables through next-to-next-to-leading order in QCD*, *JHEP* **05** (2026) 245, arXiv:2512.19613 [hep-lat].

[38] M. Dalla Brida and M. Lüscher, *SMD-based numerical stochastic perturbation theory*, *Eur. Phys. J. C* **77** no. 5, (2017) 308, arXiv:1703.04396 [hep-lat].

[39] R. Larsen, S. Mukherjee, P. Petreczky, H.-T. Shu, and J. H. Weber, *Scale Setting and Strong Coupling Determination in the Gradient Flow Scheme for 2+1 Flavor Lattice QCD*, arXiv:2502.08061 [hep-lat].

[40] M. Dalla Brida and A. Ramos, *The gradient flow coupling at high-energy and the scale of SU(3) Yang–Mills theory*, *Eur. Phys. J. C* **79** no. 8, (2019) 720, arXiv:1905.05147 [hep-lat].

[41] R. Harlander, *The gradient flow at higher orders in perturbation theory*, *PoS* **LATTICE2021** (2022) 489, arXiv:2111.14376 [hep-lat].

[42] A. Hasenfratz, C. T. Peterson, J. van Sickle, and O. Witzel, Λ *parameter of the SU(3) Yang-Mills theory from the continuous* β *function*, *Phys. Rev. D* **108** no. 1, (2023) 014502, arXiv:2303.00704 [hep-lat].

[43] Y. Kluth, *Fixed points of quantum gravity from dimensional regularization*, *Phys. Rev. D* **111** no. 10, (2025) 106010, arXiv:2409.09252 [hep-th].

[44] L. Georg, R. V. Harlander, and R. H. Mason, *The gradient-flow coupling of three-and four-dimensional QED*, *Phys. Rev. D* **113** no. 7, (2026) 076016, arXiv:2601.13914 [hep-ph].

[45] K. Falls, D. F. Litim, K. Nikolakopoulos, and C. Rahmede, *Further evidence for asymptotic safety of quantum gravity*, *Phys. Rev. D* **93** no. 10, (2016) 104022, arXiv:1410.4815 [hep-th].

[46] R. S. Hamilton, *Three-manifolds with positive Ricci curvature*, *Journal of Differential Geometry* **17** (1982) 255–306.

[47] G. Perelman, *Finite extinction time for the solutions to the Ricci flow on certain three-manifolds*, arXiv:math/0307245.

PoS(LL2026)062

[48] G. Perelman, *The Entropy formula for the Ricci flow and its geometric applications*, arXiv:math/0211159.

[49] G. Perelman, *Ricci flow with surgery on three-manifolds*, arXiv:math/0303109.

[50] R. V. Harlander, Y. Kluth, J. T. Kohnen, and H. Werthenbach, *The perturbative Ricci flow in gravity*, arXiv:2604.18678 [hep-th].

[51] H. Makino and H. Suzuki, *Lattice energy–momentum tensor from the Yang–Mills gradient flow—inclusion of fermion fields*, *PTEP* **2014** (2014) 063B02, arXiv:1403.4772 [hep-lat]. [Erratum: PTEP 2015, 079202 (2015)].

[52] A. Baldazzi, K. Falls, Y. Kluth, and B. Knorr, *Robustness of the derivative expansion in asymptotic safety*, *Phys. Rev. D* **113** no. 2, (2026) 026005, arXiv:2312.03831 [hep-th].

[53] J. Ambjørn, *Lattice Quantum Gravity: EDT and CDT*. 2024. arXiv:2209.06555 [hep-lat].

[54] J. Ambjørn and R. Loll, *Causal Dynamical Triangulations: New Lattice Theory of Quantum Gravity*, 4, 2026. arXiv:2604.05641 [hep-th].

[55] Ò. L. Crosas and P. Stoffer, *One-loop matching of the LEFT to the QCD gradient flow*, *JHEP* **07** (2026) 047, arXiv:2601.18883 [hep-ph].

[56] J. Borgulat, N. Felten, R. Harlander, and J. T. Kohnen, *Two-loop gradient-flow renormalization of scalar QCD*, *SciPost Phys. Core* **8** (2025) 032, arXiv:2501.07150 [hep-ph].

PoS(LL2026)062